CORA Cork Open Research Archive
Cartlann Taighde Oscailte Chorcaí

UCC Library and UCC researchers have made this item openly available. Please let us know how this has helped you. Thanks!

Title	Wind resource evolution in Europe under different scenarios of climate change characterised by the novel shared socioeconomic pathways
Author(s)	Martinez Diaz, Abel; Iglesias, Gregorio
Publication date	2021-04
Original citation	Martinez Diaz, A. and Iglesias, G. (2021) 'Wind resource evolution in Europe under different scenarios of climate change characterised by the novel Shared Socioeconomic Pathways', Energy Conversion and Management, 234, 113961 (16pp). doi:10.1016/j.enconman.2021.113961
Type of publication	Article (peer-reviewed)
Link to publisher's version	http://dx.doi.org/10.1016/j.enconman.2021.113961 Access to the full text of the published version may require a subscription.
Rights	**© 2021 The Author(s). Published by Elsevier Ltd. This is an open access article under the CC BY license e (http://creativecommons.org/licenses/by/4.0/)** https://creativecommons.org/licenses/by/4.0/
Item downloaded from	http://hdl.handle.net/10468/13102

Downloaded on 2022-05-18T19:22:57Z

UCC
University College Cork, Ireland
Coláiste na hOllscoile Corcaigh

Energy Conversion and Management 234 (2021) 113961

Contents lists available at ScienceDirect

Energy Conversion and Management

journal homepage: www.elsevier.com/locate/enconman

Wind resource evolution in Europe under different scenarios of climate change characterised by the novel Shared Socioeconomic Pathways

A. Martinez [a], G. Iglesias [a,b,*]

[a] MaREI, Environmental Research Institute & School of Engineering, University College Cork, College Road, Cork, Ireland
[b] University of Plymouth, School of Engineering, Marine Building, Drake Circus, Plymouth PL4 8AA, United Kingdom

ARTICLE INFO

Keywords:
Wind energy
Wind power
Climate change
Renewable energy
Muli-model ensemble
Shared socioeconomic pathway

ABSTRACT

Wind energy is a fundamental pillar of the energy mix in Europe – hence the need for understanding the evolution of the wind energy resource under climate change. For this purpose, near-, mid- and long-term wind speed projections from 18 global climate models are considered and a multi-model ensemble is constructed with the ones found to best reproduce past-present conditions. The evolution and temporal variability of wind power is investigated considering different climate change scenarios through the novel Shared Socioeconomic Pathways (SSPs). More specifically, two SSPs are considered, each corresponding to its own socio-economic and political environment and, therefore, its own level of greenhouse emissions: SSP5-8.5 (highest emissions scenario) and SSP2-4.5 (intermediate emissions scenario). Both scenarios lead to a significant reduction (up to 35%) in wind power density in northern Continental Europe and the Central Mediterranean, and an increase of similar magnitude in West Finland. Over the Atlantic Ocean, Ireland and Britain the resource is also projected to decrease significantly. In other regions, however, the general trend (positive or negative) depends on the SSP scenario. This is the case, notably, of Central Europe, with considerable growth in SSP2-4.5 but some reduction in SSP5-8.5. Thus, in the intermediate emissions scenario (SSP2-4.5) both growth and decline in wind power density are forecast, depending on the region. By contrast, in the highest emissions scenario (SSP5-8.5) the forecast is a general decrease, of the order of 15% overall, with an annual rate of change of approximately –0.2% and an increase in seasonal variability. These trends will affect the energy production of wind farms and, therefore, need to be accounted for in assessing wind power projects in Europe.

1. Introduction

The combustion of fossil fuel for energy production has been proven to be one of the main causes of climate change [1]. The European Commission's strategy acknowledges the urgency of reducing the emission of greenhouse gases (GHG) and calls for a significant increase in renewable energy capacity. Thanks to its technological and commercial maturity, wind power can really make a difference in advancing the European Commission's strategy.

In 2019, 15.4 GW of new wind power capacity was installed in Europe, which represents a hefty 27% increase on the previous year [2]. At the end of the year, the total wind power capacity installed in Europe was 205 GW, covering 15% of the energy demand in the European Union. This means that the ambitious goals set by the European Energy Commission [3] can only be reached by expanding wind power capacity and, to a lesser extent, by improving the efficiency of already installed devices [4]. Recently, the scope of wind energy has been broadened by the strong development of offshore wind [5] – a record 3.3 GW of new offshore wind power capacity was installed in 2019 in Europe [2]. Research on new technological solutions for wind energy includes its combination with other resources such as: wave energy [6], with offshore devices mounted on monopiles [7] or jacket structures [8]; solar [9]; or the more complex wind–solar–fossil energy system [10]. As a result, areas not yet exploited may become suitable for future wind energy development [11]. Furthermore, in the last years, small islands which are still overly dependent on fossil fuels and energy imports have found in both onshore and offshore wind energy a great alternative in the quest for energy self-sufficiency, both for onshore [12] and offshore wind [13], e.g., Naxos [14]. The potential of hybrid wave-wind energy systems [15] has been also investigated for small islands [16]. In Europe, examples can be found in Tenerife [17], Fuerteventura [18] or the Aegean Sea [19]. With all these new trends in the wind energy market,

* Corresponding author at: MaREI, Environmental Research Institute & School of Engineering, University College Cork, College Road, Cork, Ireland.
E-mail address: gregorio.iglesias@ucc.ie (G. Iglesias).

https://doi.org/10.1016/j.enconman.2021.113961
Received 23 October 2020; Received in revised form 23 October 2020; Accepted 13 February 2021
Available online 7 March 2021
0196-8904/© 2021 The Author(s). Published by Elsevier Ltd. This is an open access article under the CC BY license (http://creativecommons.org/licenses/by/4.0/).

the assessment of the mid- and long-term evolution of the wind resource is essential with a view to laying the foundations for future investments in wind energy.

Wind power is especially sensitive to variations in wind patterns – indeed, it is proportional to the cube of wind speed, and therefore small fluctuations in wind speeds are greatly amplified in wind power. With atmospheric flow patterns predicted to change due to increased GHG emissions [20], it is crucial to take into account the impact of climate change on the future development of wind energy. The first works addressing the evolution of wind under climate change in Europe are based on climate change scenarios A2 and B2 of cumulative GHG emissions [21], developed by the Intergovernmental Panel on Climate Change (IPCC) in the IPCC Third Assessment Report (TAR) [22].The first thorough assessments of wind speed and wind energy in Europe were presented for Northern Europe [23] and Eastern Mediterranean [24], focusing on the long-term (2071–2100) evolution. More recently, a number of models were applied to investigate the impact of climate change in the European wind energy resource [25] and the effects in wind power production [26]. Regional works addressing future changes in wind energy can be found for the UK [27] and Ireland (using the RCA3 [28] and the COSMO-CLM [29] climate models). Generally speaking, wind speeds are predicted to increase weakly in Northern Europe and decrease slightly in Southern Europe and the Central Mediterranean. However, wind speeds appear to be very sensitive to the choice of global climate model (GCM) and initial conditions. The evolution of the wind power density [30] and the energy output of a benchmark turbine [31] over Europe under climate change are studied using an ensemble of GCMs available through the 5th phase of the Coupled Model Intercomparison Project (CMIP5), which uses the Representative Concentration Pathways (RCPs) [32]. By using different ensemble techniques, both show similar results for the Baltic countries, although the models disagree strongly regarding the wind energy evolution in Central Europe.

Recently, an extensive ensemble of GCMs and Earth System Models (ESMs) has been made available by the 6th phase of the Coupled Model Intercomparison Project (CMIP6) [33]. The Scenario Model Intercomparison Project (ScenarioMIP) [34] occupies a prominent position among the activities covered in this phase and provides climate projections based on new alternative scenarios of future GHG emissions and land use [35]. These updated scenarios are produced with integrated assessment models (IAMs) and driven by the updated pathways of societal development, the Shared Socioeconomic Pathways (SSPs) [36].

So far the evolution of the wind energy resource has not been studied using the SSPs. Moreover, the intra-annual variability (seasonality) of the wind energy resource is seldom studied in previous works, possibly due to the limited frequency of the data – typically, monthly averaged values are used. However, some regions present significant intra-annual variability. This is the case, notably, of the Atlantic European shores, which are subject to strong winds from extratropical cyclones [37]. While the economic viability of a wind farm depends to a great extent on the mean values of wind speed, the intra-annual variability plays an important role in balancing supply-demand in the electricity grid, ultimately affecting the profitability of the farm [38].

In this work, the most recent climate change projections based on the SSPs case scenarios are employed to assess the near-, mid- and long-term trends of wind energy in Europe. The repercussions of the latest climate projections on wind power density, derived from the near-surface wind speed data from the GCMs involved in the CMIP6 activities, are studied by comparison with past-present data. Furthermore, daily data on wind speed are used to assess the effects of climate change on the evolution of the intra-annual variability, of interest given the seasonality of the European wind resource.

Table 1
GCMs considered in this work.

Model	Centre	Resolution (lat × lon)	References
AWI-CM-1-1-MR	Alfred Wegener Institute (Germany)	0.9375° × 0.9375°	[40]
BCC-CSM2-MR	Beijing Climate Center (China)	1.12° × 1.125°	[41]
FGOALS-f3-L	Chinese Academy of Sciences (China)	1° × 1.25°	[42]
CanESM5	Canadian Centre for Climate Modelling and Analysis (Canada)	1.775° × 2.1825°	[43]
ACCESS-CM2	Commonwealth Scientific and Industrial Research Organisation (Australia)	1.25° × 1.875°	[44]
MPI-ESM1-2-HR	Max Planck Institute for Meteorology (Germany)	0.93° × 0.9375°	[45]
MPI-ESM1-2-LR	Max Planck Institute for Meteorology (Germany)	1.85° × 1.875°	[46,47]
EC-Earth3	EC-EARTH-CONSORTIUM (Europe)	0.7° × 0.7031°	[48]
INM-CM4-8	Institute for Numerical Mathematics (Russia)	1.5° × 2°	[49,50]
INM-CM5-0	Institute for Numerical Mathematics (Russia)	1.5° × 2°	[51,52]
IPSL-CM6A-LR	Institut Pierre Simon Laplace (France)	1.2676° × 2.5°	[53]
MIROC6	JAMSTEC (Japan Agency for Marine-Earth Science and Technology) (Japan)	1.4° × 1.4063°	[54]
MRI-ESM2-0	Meteorological Research Institute (Japan)	1.12° × 1.125°	[55]
CESM2-WACCM	National Center for Atmospheric Research (USA)	0.9424° × 1.25°	[56]
NorESM2-MM	NorESM Climate modeling Consortium (Norway)	0.9424° × 1.25°	[57]
KACE-1-0-G	National Institute of Meteorological Sciences/Korea Meteorological Administration (Republic of Korea)	1.25° × 1.875°	[58]
GFDL-CM4	NOAA-GFDL (USA)	1° × 1.25°	[59]
GFDL-ESM4	NOAA-GFDL (USA)	1° × 1.25°	[60]

The present paper proceeds as follows. First, historical near-surface wind speed data from the 18 GCMs considered in this work are compared with reanalysis data to select the GCMs that better represent past-present wind speeds. On this basis, data from the selected GCMs are assembled in a multi-model ensemble and future trends of mean wind power density and intra-annual variability over Europe are assessed.

2. Materials and methods

The data used in this work derive from the GCMs framed in the CMIP6 activities. Future climate projections within the ScenarioMIP activity are used and compared with data from CMIP historical simulations to assess changes in the wind energy resource. In this study, daily mean near-surface wind speed data over Europe are used – more specifically, the ranges of latitude and longitude considered are (26°N, 72°N) and (26°W, 40°E), respectively. Following standard practice in this type of study, near-surface (10 m height) wind data are used as the reference. Wind speeds at different heights may be determined by means of the Hellman exponent and wind gradient equation [39].

Two different climate change scenarios are considered in the projections of wind speed: SSP5-8.5 and SSP2-4.5 [34]. SSP5-8.5 represents an extreme scenario in which no policies are applied regarding the emission of GHGs, i.e. with intensive fossil-fuel consumption resulting in a forcing pathway of 8.5 Wm^{-2} in 2100. On the contrary, SSP2-4.5 is an intermediate scenario, in which current climate change trends continue without substantial deviations, leading to a forcing pathway of 4.5

Table 2
Number of points in the grid statistically similar to their ERA-5 counterparts (percentage of total number of points).

Model	Number of grid points statistically similar
EC-Earth3	67%
GFDL-CM4	67%
NorESM2-MM	66%
CESM2-WACCM	64%
GFDL-ESM4	62%
IPSL-CM6A-LR	58%
FGOALS-f3-L	56%
ACCESS-CM2	52%
MPI-ESM1-2-HR	50%
CanESM5	50%
AWI-CM-1-1-MR	50%
BCC-CSM2-MR	47%
MIROC6	45%
MPI-ESM1-2-LR	44%
INM-CM4-8	44%
MRI-ESM2-0	43%
INM-CM5-0	43%
KACE-1-0-G	39%

Wm^{-2} by 2100.

In this study, the 18 GCMs involved in the CMIP6 activities that provide future projections of daily averaged near-surface wind speed data in both case scenarios, SSP2-4.5 and SSP5-8.5, are considered (Table 1).

2.1. Validation of the data

The data are compared and validated using the up-to-date ERA-5 reanalysis database from the European Centre for Medium-Range Weather Forecasts (ECMWF) [61]. The ERA-5 database is chosen for two reasons: (i) it is the most recognised database in reanalysis products, widely used as a reference in other analyses [62], and (ii) the ERA products have been the official validation datasets for the CMIP downscaling initiatives [63]. Besides, they have been widely used for validation by previous works [64]. Near-surface wind speed historical data (2005–2014) of the GCMs listed in Table 1 are compared to the ERA-5 near-surface wind speed data in the same period.

In the following, the wind speed projections obtained with each GCM are compared to the historical data computed with the same GCM. It is therefore of interest for the scope of this paper to evaluate distributional differences of the GCMs rather than the mean differences (biases) to determine reanalysis uncertainties. To assess distributional differences, the two-sample Kolmogorov-Smirnov test is employed (K-S test), which examines the null hypothesis of two different sample data belonging to the same distribution against the alternative that they are not [65].

First, since the GCMs employed in this work have different native resolutions (Table 1), all the GMCs are remapped into a regular grid, which is chosen to be $1.5^\circ \times 1.5^\circ$ using a first-order conservative remapping, maintaining the flux integrals [66]. Since daily data on atmospheric sciences are largely seasonal-dependent, the K-S test is applied to the time series centred to have zero mean, obtained by subtracting the seasonal mean (bias) in each time step. Eliminating the bias of the time series before applying the K-S test has been proved to detect distributional differences in higher-order moments, and it is a common practice in downscaling approaches [67]. The two-sample K-S test is applied to the unbiased time-series data of the GCMs listed in Table 1 against the unbiased time series ERA-5 data covering the same period at a significance level of 5%. The number of points in the grid which are statistically similar to their ERA-5 counterparts is shown in Table 2 as a percentage of the total number of points.

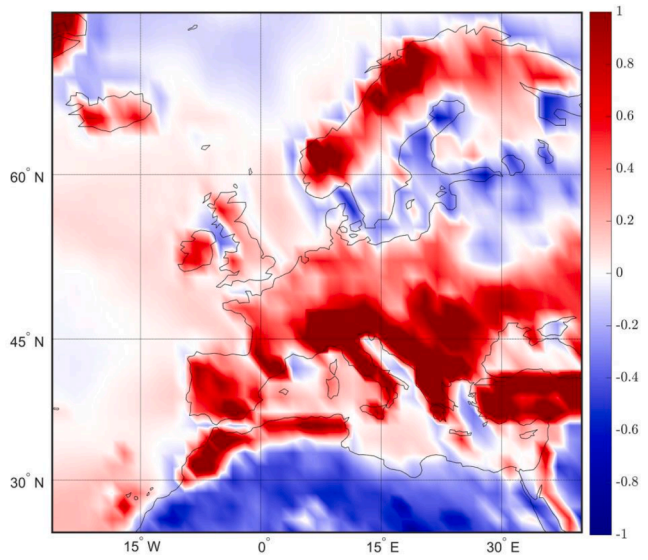

Fig. 1. Normalised bias of the historical data of the multi-model ensemble relative to the ERA-5 time series.

2.2. Methods

In order to assess the evolution of the wind energy resource using the CMIP6 projections of daily wind speed, a multi-model ensemble (MME) of the GCMs that represent the most statistically accurate historical data is constructed [68]. It has been shown that, by using the MME approach, individual uncertainties are eliminated, therefore producing more reliable results than single-model approaches [69]. In this work, GCMs with higher percentages of statistically similar grid points to the ERA-5 dataset are selected for the multi-model ensemble. More specifically, the GCMs with more than 62% of statistically similar grid points are chosen, namely: EC-Earth3, GFDL-CM4, NorESM2-MM, CESM2-WACCM and GFDL-ESM4 (Table 2). These GCMs are integrated into an MME following an un-weighted approach [70].

Three periods are considered for the projections: the near-term future (2021–2030), mid-term future (2056–2065) and long-term future (2091–2100). Time periods of ten years were selected as a compromise between temporal resolution and the need to avoid spurious influences from hyperannual variation cycles. The MME is computed for the three periods under the two climate change scenarios considered and the results are compared against the historical MME data counterpart (2005–2014), which is referred to hereinafter as the Baseline. The comparison is made by subtracting the Baseline value from the projected value and expressing the result as a percentage of the Baseline value.

First, the mean difference (bias) of the historical MME and the ERA-5 in the same period is studied. Since the variability of the time series depends to a great extent on the latitude, the bias is normalised against the standard deviation of the sample [67] (Fig. 1). Overall, the MME approach shows good agreement with the ERA-5 time series, especially over large water bodies. Near-surface winds are influenced by orographic features, which cannot be fully captured by either model due to their coarse spatial resolution. Consequently, some discrepancies are to be expected, in particular over large mountain ranges, such as the Alps, Pyrenees or the Apennines.

Second, the wind power density (P) is calculated as

$$P = \frac{1}{2}\rho U^3, \tag{1}$$

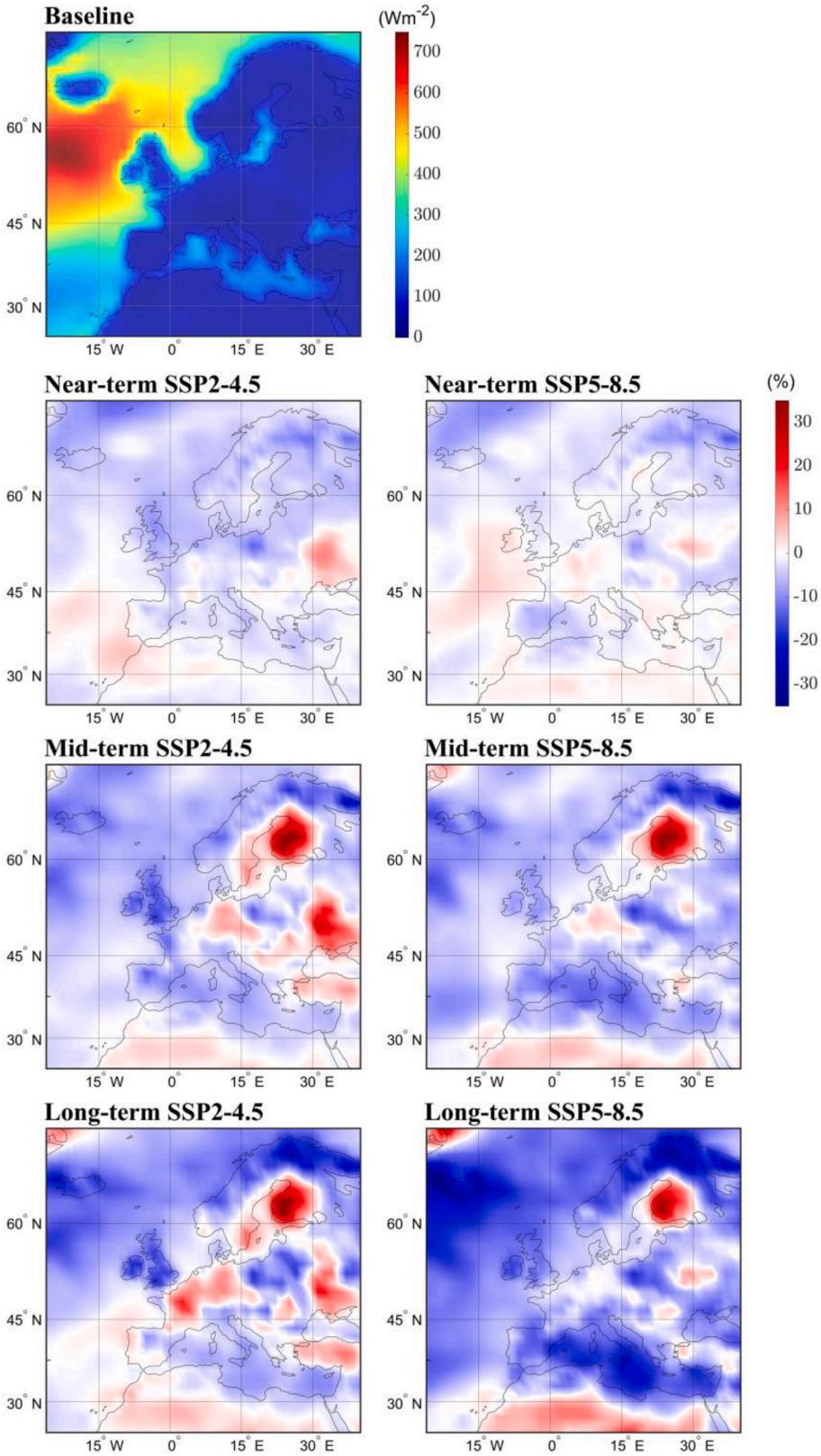

Fig. 2. Evolution of mean wind power density in Europe. Historical values (Baseline) of mean wind power density (Wm^{-2}, uppermost panel) and change (%) relative to the historical values in the near-, mid- and long-term future for climate change scenarios SSP2-4.5 (left) and SSP5-8.5 (right).

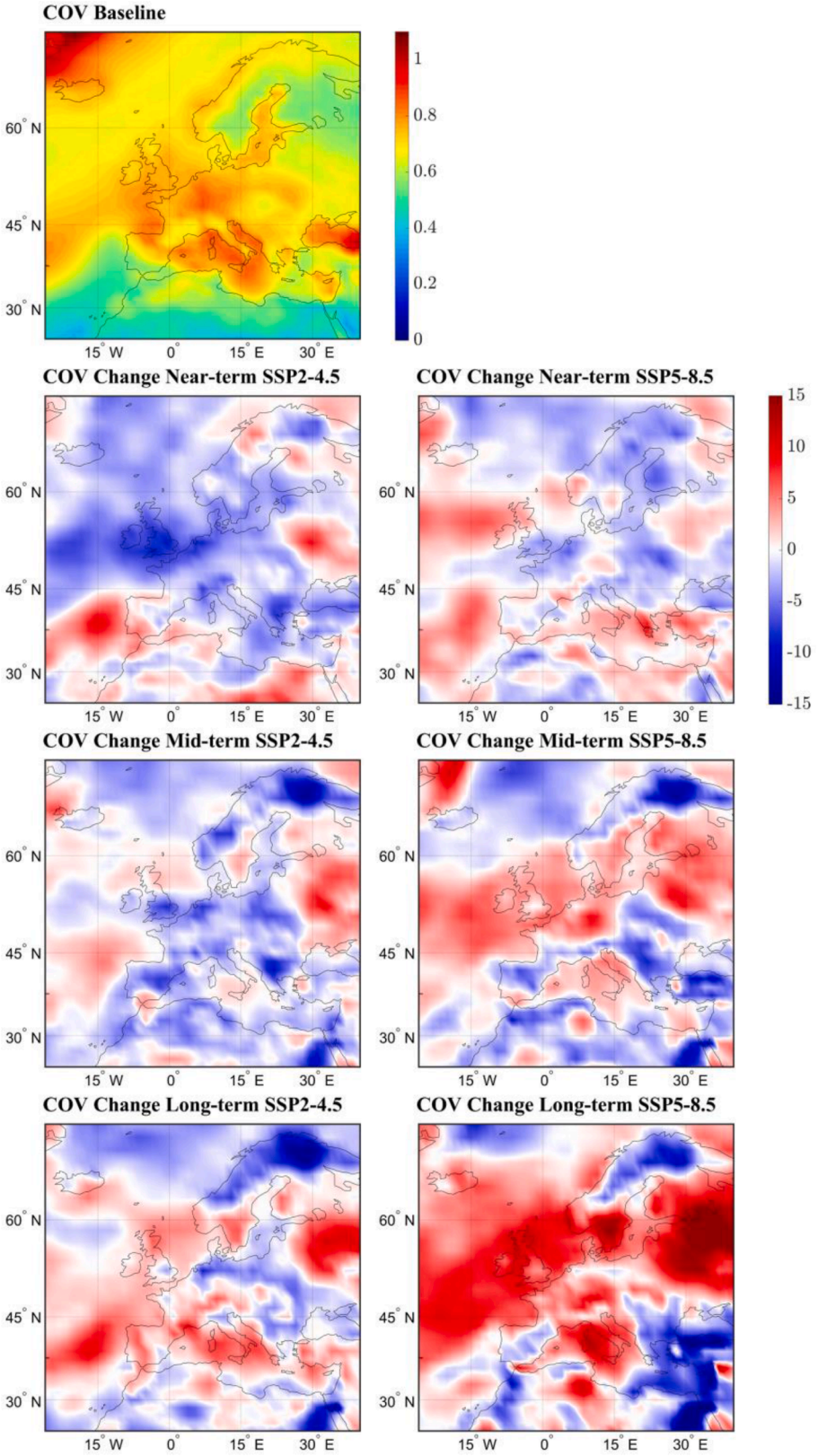

Fig. 3. Evolution of the coefficient of variation (COV) in Europe. Historical values of the COV (uppermost panel) and change (%) in the COV in the near-term, mid-term and long-term time, for SSP2-4.5 (left) and SSP5-8.5 (right) scenarios of climate change.

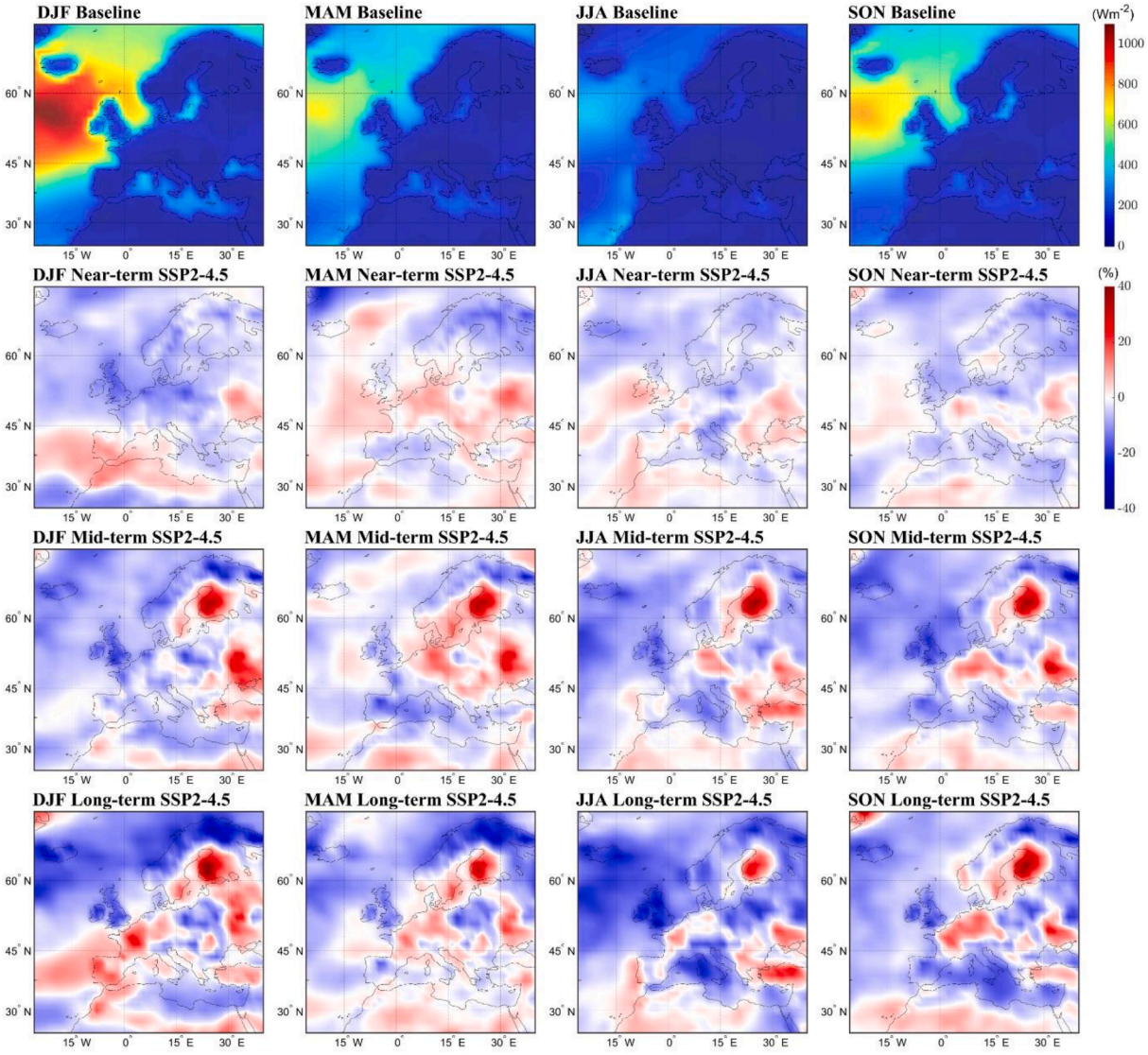

Fig. 4. Evolution of the seasonal mean wind density in Europe under SSP2-4.5 climate change scenario. The historical seasonal mean wind power density (Wm^{-2}) is displayed on the first (uppermost) row of panels, and the change (%) in the near-term, mid-term and long-term periods is depicted on the second, third and fourth row, respectively.

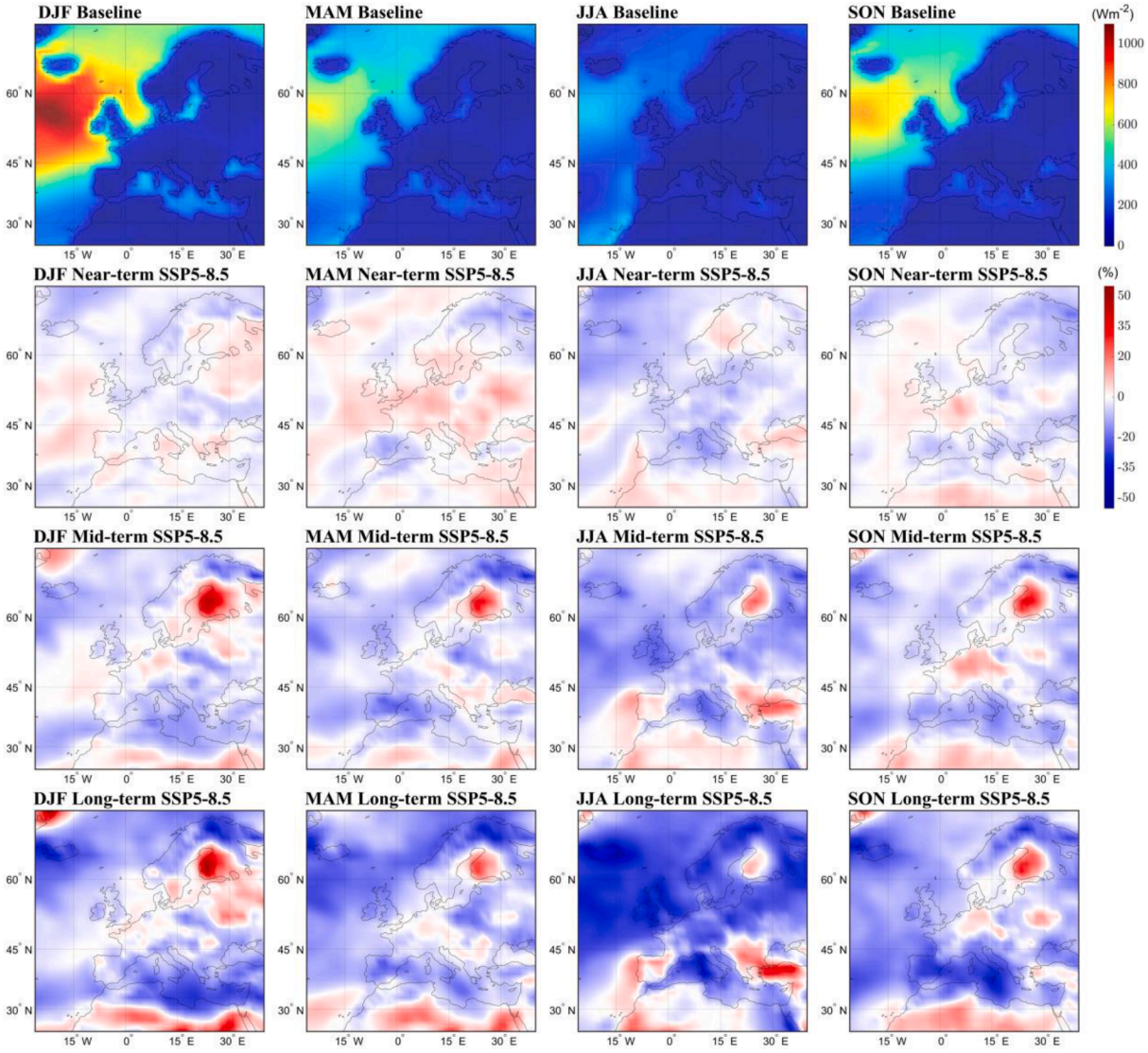

Fig. 5. Evolution of the seasonal mean wind density in Europe under SSP5-8.5 climate change scenario. The historical seasonal mean wind power density (Wm^{-2}) is displayed on the first (uppermost) row of panels, and the change (%) in the near-term, mid-term and long-term periods is depicted respectively on the second, third and fourth row.

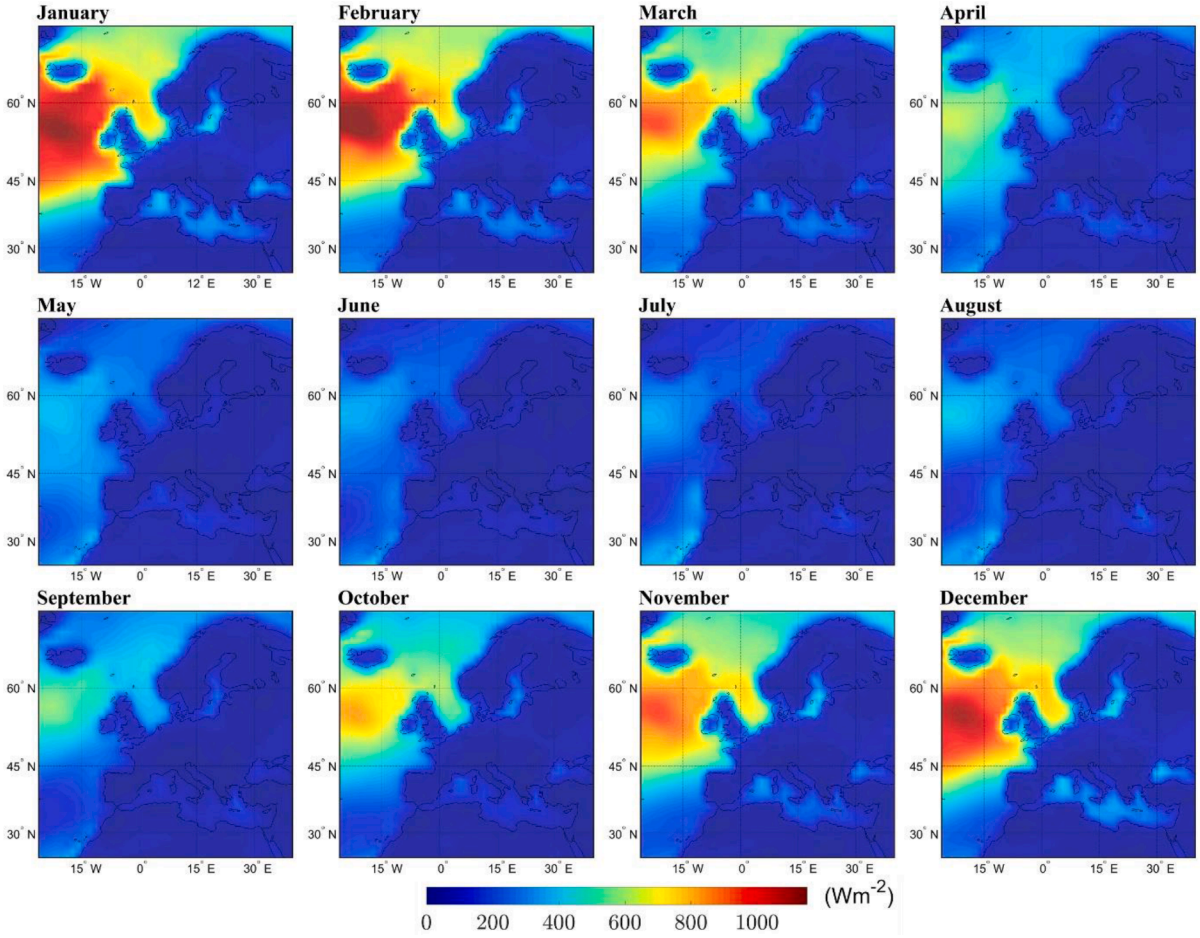

Fig. 6. Monthly mean wind power density in the Baseline period (Wm^{-2}).

where U is the wind speed and ρ is the air density, taken to be 1.225 kgm^{-3}. Given the cubic relationship between P and U in Eq. (1), small fluctuations in the wind speed are greatly amplified in the wind power density.

3. Results and discussion

With the wind speed data and methods presented in Section 2, the multi-model ensemble data of daily-averaged near-surface wind power density are computed using Eq. (1). Values of the mean wind power density and temporal variability are calculated and compared with the Baseline to study the evolution of the resource.

3.1. Mean wind power density

Mean values of wind power density for the near-, mid- and long- term future are calculated and compared with the Baseline (Fig. 2). The highest wind power densities occur near the 55th parallel, close to the west of Ireland and south of Iceland, with mean wind power density values over 700 Wm^{-2} provided by the prevailing westerlies. Closer to the continental landmass, the Bay of Biscay and the North and Norwegian Seas display values around 450 Wm^{-2}.

The near-term future differences from the Baseline are below ± 10% in both climate change scenarios (Fig. 2). Notwithstanding, differences of up to 10% are not necessarily negligible given the proximity between the near-term future (2021–2030) and the Baseline (2005–2014). Differences with respect to the Baseline are significantly greater in the mid-term (2056–2065) and long-term future (2091–2100). Moreover, given a certain climate change scenario, differences between the mid-term future and the Baseline are generally of a similar magnitude and sign as differences between the long-term and mid-term future.

Importantly, in the climate change scenario with the highest GHG emissions, SSP5-8.5, a widespread decrease in the European wind power density is predicted. The greatest reductions in wind power density are projected in Britain, Ireland and the northernmost regions of the continent (Northern Norway and the Finnish Lapland), in the range of 20–35%. A general decrease up to 25% is also predicted in the Mediterranean Sea, in agreement with other studies [31]. An interesting nuance is that in work this reduction of wind power density appears to be more pronounced in the Italian Peninsula. Overall, the SSP5-8.5 predicts a general decrease in wind power density of approximately 15% in the long-term future, which is equivalent to roughly 0.2% annually.

In the intermediate climate change scenario, SSP2-4.5, a general trend that would hold generally for the entire continent cannot be discerned. Instead, the evolution of the resource presents regional differences. Significant decreases in wind power density are projected for Ireland, Britain, the Mediterranean Sea and the northernmost regions of the continent (in the range of 10–30%).

Some discrepancies are observed between the projections in different climate change scenarios, including in some cases even opposite trends at regional level. This is the case, most notably, of Central Europe and parts of Western Europe (France, Germany, Czech Republic), where the SSP2-4.5 scenario predicts a rise of up to 15% in wind power density, while the SSP5-8.5 scenario projects slight reductions. These discrepancies indicate that some regions are highly sensitive to the climate change scenario, which may well be the reason behind the discrepancies found in the literature on the evolution of wind energy in Central Europe

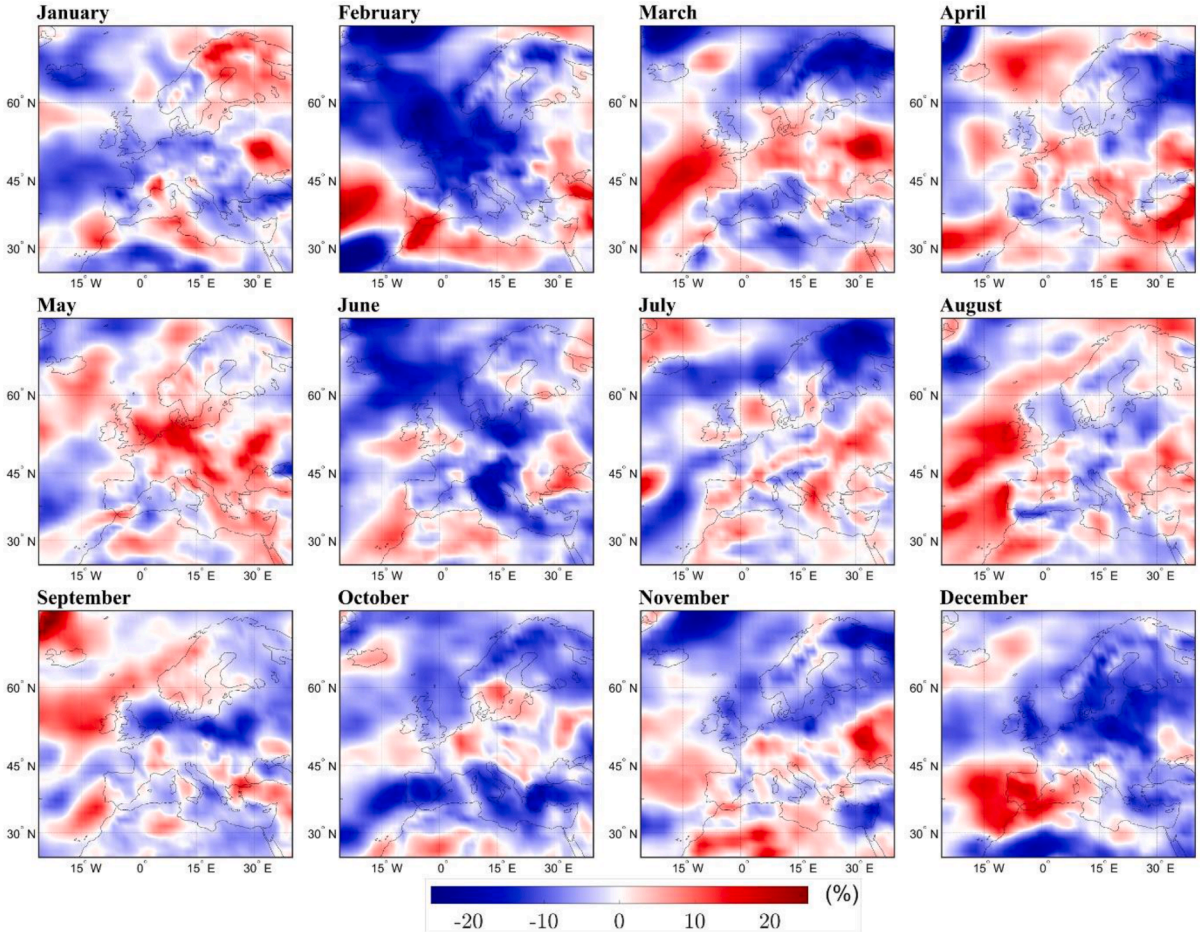

Fig. 7. Evolution (%) of the monthly mean wind power density in the near-term future under SSP2-4.5 climate change scenario.

[25,30,31]. Other strong discrepancies between climate change scenarios are found in Turkey and Ukraine.

Finally, both climate change scenarios agree in predicting a substantial increase (of the order of 30%) in wind power density in Western Finland. Despite the generally constant rate of change of wind power density, this increase takes place mostly between the near- and mid-term future, with little change thereafter. Interestingly, a slight growth in wind energy around the Baltic countries is mentioned in other studies [71]; however, the increase predicted in this work is more substantial, and located entirely over the landmass.

3.2. Variability

The variability of the wind power density is studied by means of the coefficient of variation (*COV*) [72], which is the ratio of the standard deviation, σ, to the mean value, $\overline{x}$, of a statistical sample,

$$COV = \frac{\sigma}{\overline{x}}. \quad (2)$$

The coefficient of variation is computed for the historical database of the MME and the near-term, mid-term and long-term future projections for both scenarios of climate change, i.e., SSP2-4.5 and SSP5-8.5 (Fig. 3).

In the Baseline, the wind energy resource is most variable in the Bay of Biscay, Germany, the Mediterranean Sea (in particular, the Tyrrhenian and Adriatic Seas) and the Black Sea. In Northern Europe, the most stable wind energy resource is found in Sweden and West Finland, whereas in the southern regions it is located below the 45th parallel in the Atlantic Ocean and off Portugal.

An overall growth in the variability of wind energy in Europe is predicted in both climate change scenarios, which increases over time. The greatest variability is observed in climate change scenario SSP5-8.5, which predicts a widespread increase in the *COV* over 10% in offshore and Central Europe.

A significant increase in variability is projected in the Atlantic Ocean, Ireland and Britain (>10% in the SSP5-8.5 scenario), the southernmost parts of Sweden and Norway (>15%), the Baltic Countries, Belarus and West Russia (>15%) and the Mediterranean Sea (up to 15%). Central Europe and West Finland exhibit a smaller but still noticeable increase in the range 5–10%.

On the other side, a notable reduction in variability (of around 10%) is predicted in the northernmost regions of Continental Europe – Norway and, especially, the Finnish Lapland.

3.3. Intra-annual variability: Seasonal mean wind power density

To assess the evolution of the intra-annual variability, the seasonal mean wind power density is calculated and compared with the Baseline for climate change scenarios SSP2-4.5 and SSP5-8.5 (Figs. 4 and 5, respectively). The year is divided into three-month periods, i.e., December – January – February (DJF), March – April – May (MAM), June – July – August (JJA) and September – October – November (SON).

In the Baseline, the pronounced seasonality of the wind energy resource in the European Atlantic is apparent, with the highest values in SON and DJF, matching the extratropical cyclones season. The most energetic winds occur in the upper-mid latitudes in DJF, with mean wind power densities topping 1100 Wm^{-2} – in stark contrast with JJA, when they remain below 450 Wm^{-2}.

The evolution of wind power density in climate change scenario

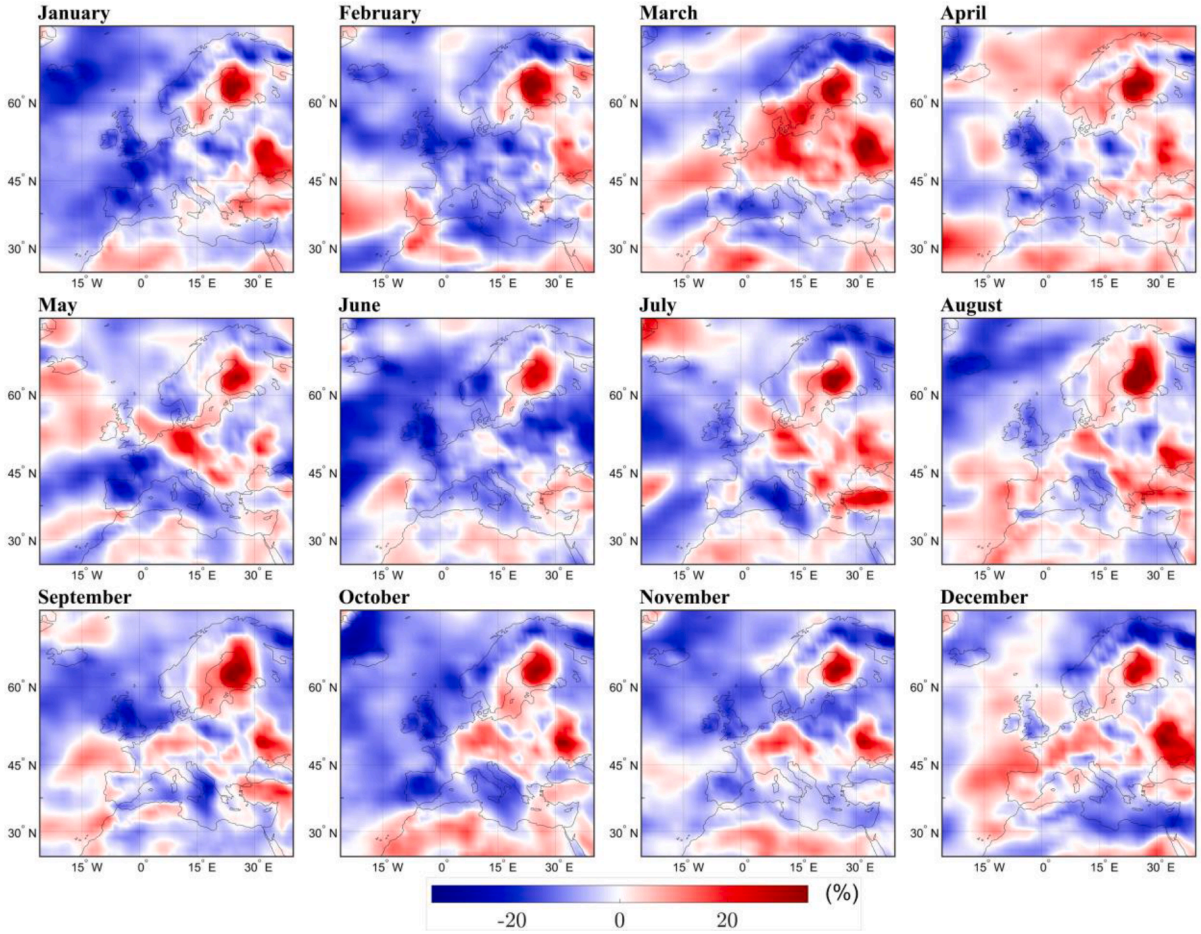

Fig. 8. Evolution (%) of the monthly mean wind power density in the mid-term future under SSP2-4.5 climate change scenario.

SSP2-4.5 (Fig. 4) presents considerable seasonality in the Iberian Peninsula and the surrounding Atlantic Ocean. In the long-term future, increases in wind power density of ~15% and ~10% occur in DJF and JJA, whereas a general decrease is projected in MAM and SON. The evolution of the resource also presents considerable seasonal variability in the Central Mediterranean, with little to no significant differences from the Baseline in DJF and MAM but substantial decreases, of up to 25%, in JJA and SON.

On the other hand, some differences from the Baseline projected in the SSP2-4.5 scenario are persistent throughout the year. A substantial increase in wind power density is projected, over 40% in Western Finland and up to 20% in Central and parts of Western Europe (France, Germany, Czech Republic, Belgium and the Netherlands) and Ukraine. On the other hand, drops in wind power density throughout the year are predicted for Ireland, Britain and the northernmost regions of the Atlantic Ocean and Continental Europe – Norway, Sweden and the Finnish Lapland, with values in the range 10–30%.

A much stronger seasonal variability is found in climate change scenario SSP5-8.5 (Fig. 5). Decreases in wind power density up to 35% are projected in JJA in Central Europe and the upper-mid latitudes of the Atlantic Ocean, including Ireland, Britain and Iceland, whereas the rest of the year changes remain below ± 10%, in agreement with other works in literature [25]. The opposite trend is observed in the Iberian and Balkan Peninsula, which present in JJA a significant increase in wind power density of 15% and 30%, respectively. However, changes in wind energy density are below 10% the rest of the year. Non-seasonal variability in the SSP5-8.5 is observed in the Central Mediterranean, which presents a decrease of up to 35% in wind power density.

3.4. Intra-annual variability: Monthly mean wind power density

The monthly mean wind power density is computed and compared to historical data to assess the intra-annual evolution of the wind energy resource in the near-term, mid-term and long-term future for climate change scenarios SSP2-4.5 and SSP5-8.5.

Substantial changes in wind power density relative to the Baseline (Fig. 6) are projected for the near-term future in climate change scenarios SSP2-4.5 (Fig. 7) and SSP5-8.5 (Fig. 10), of up to ± 25%. However, these changes are not consistent during the year. Even though no specific trends in the evolution of the wind energy resource can be ascertained in this period, both climate change scenarios present very similar results.

Seasonal variability is apparent in several regions in the SSP2-4.5 scenario (Figs. 8 and 9). Along the Atlantic shores of the Iberian Peninsula and the Bay of Biscay, a notable increase of 20% in wind power density is projected in December, February and March, whereas little to no significant changes are projected for the rest of the year. Considerable seasonal variability is also present in the Mediterranean

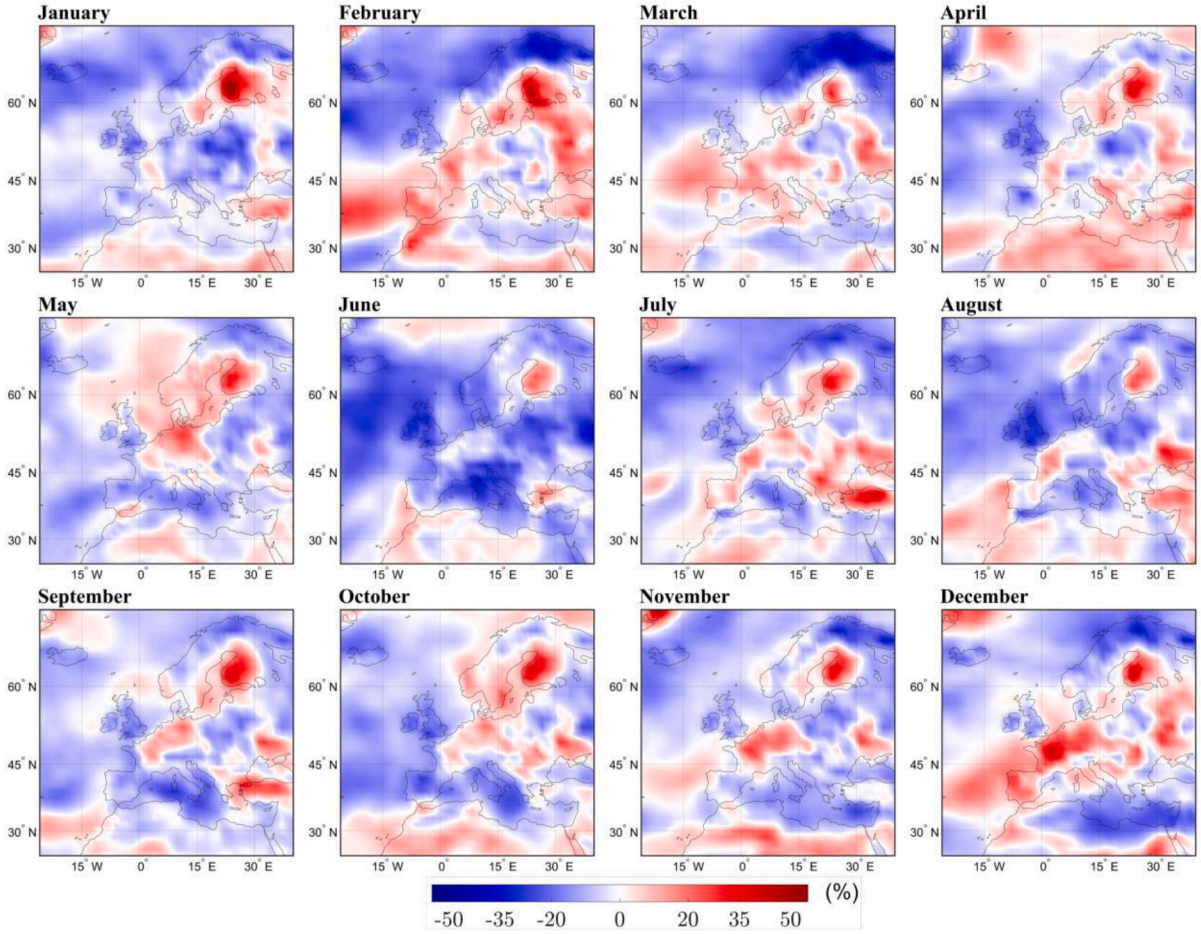

Fig. 9. Evolution (%) of the monthly mean wind power density in the long-term future under SSP2-4.5 climate change scenario.

Sea, with changes in wind power density of up to 25% exclusively from June to October. Similarly, although a general decline is predicted throughout the year in the northernmost regions of Europe, a substantial increase is predicted for February and March (>40%).

On the other side, increases in the available wind energy which are consistent throughout the year are projected in the SSP2-4.5 scenario in Central Europe and parts of Western Europe – especially in France, Germany, the Netherlands and Belgium, with peak values of ~30% in December – and West Finland – peaks over 50% occurring in January.

Importantly, a much stronger intra-annual variability is projected in climate change scenario SSP5-8.5 (Figs. 11 and 12), with no regions maintaining a consistent evolution throughout the year. Although a remarkable increase in wind energy is predicted in West Finland throughout the year, values range from approximately 10% between June and September to a much greater growth during the rest of the year – peaks of 55% in December and January. Given that historical data register the lowest values of wind energy between May and August, the variability of the resource may be expected to increase, as shown in the evolution of the *COV*.

Finally, a notable trend arises in the SSP5-8.5. This scenario predicts slight increases in wind energy in a six-month period from October to April in mid- and upper-latitude regions – above the 50th parallel. The rest of the year, however, a strong decline of 20% is predicted. In stark contrast, the opposite trend is observed in the Balkan Peninsula and, to a lesser extent, in the Iberian Peninsula, with noticeable increases in wind energy precisely from April to October (up to 40% in the Balkan Peninsula) but small decreases in the remaining six months. These intra-annual trends become more relevant when taking into account the fact that the most energetic winds occur mainly in winter, matching the extratropical cyclone season. As a result, large increases in the variability of the resource may be expected in Central and Northern Europe, in contrast with the Balkan and Iberian Peninsulas.

3.5. Discrepancies between climate change scenarios

Comparing the two climate change scenarios, it is noteworthy that the predictions for certain regions are diametrically opposed. This is the case, most notably, of much of Western and Central Europe (France, Belgium, the Netherlands, Germany, Czech Republic) where the SSP2-4.5 scenario predicts a significant increase in wind power density, whereas slight decreases are predicted in the SSP5-8.5 scenario. The sensitivity of the evolution of wind energy in these regions to the climate change scenario may be the reason behind the discrepancies in the literature in this regard.

4. Conclusions

The evolution of the European wind energy resource under the effects of climate change was investigated using a multi-model ensemble of 5 global climate models. These models were selected among 18 GCMs participating in the CMIP6 activities on the basis of their performance in modelling past-present wind flow conditions. These climate projections consider the most recent scenarios of GHG emissions and land use, driven by the novel pathways of societal development: the Shared Socioeconomic Pathways. More specifically, the SSP2-4.5 and SSP5-8.5 scenarios, representing business-as-usual and augmented emissions, respectively, are considered.

The evolution of wind energy is studied by comparing climate

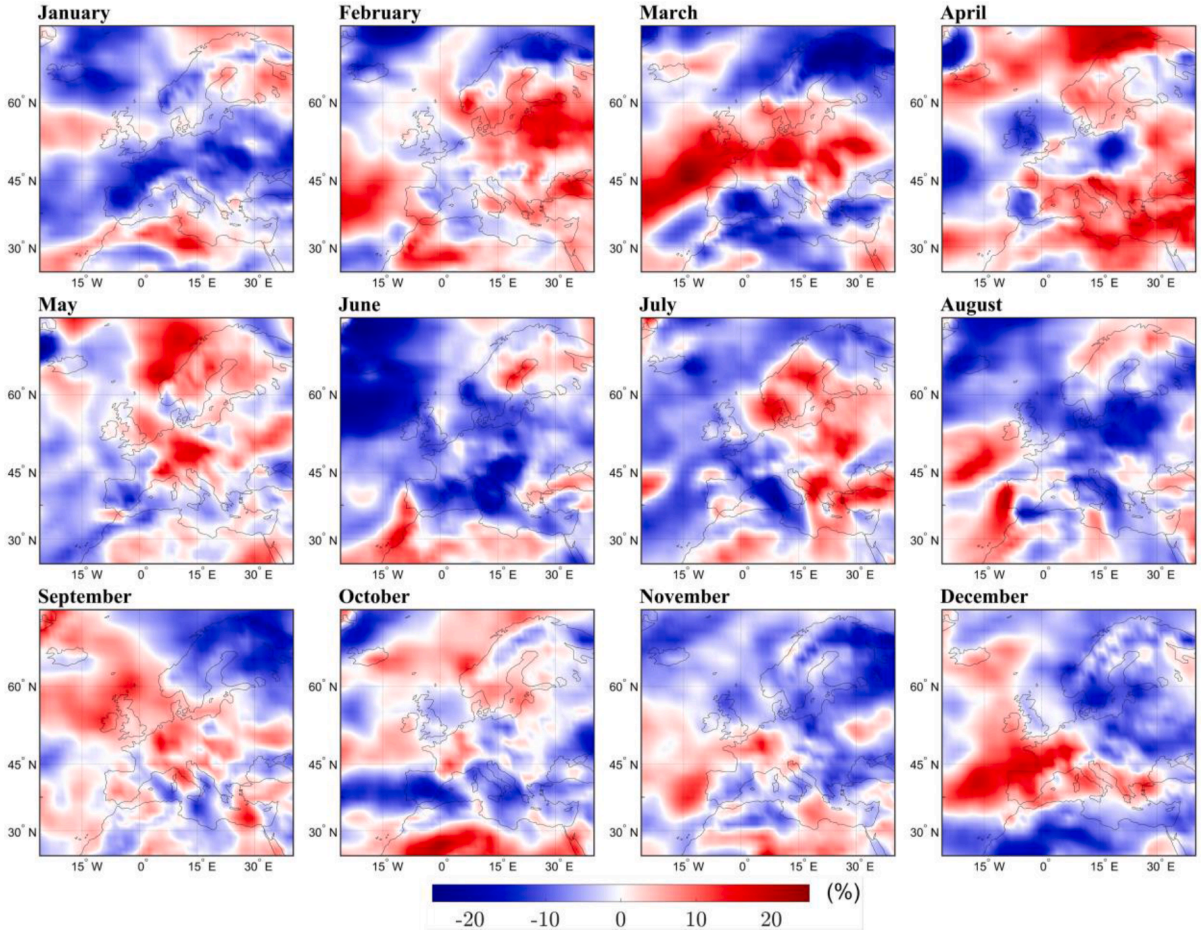

Fig. 10. Evolution (%) of the monthly mean wind power density in the near-term future under SSP5-8.5 climate change scenario.

change projections with historical data. Clear trends become apparent in the mid-term (2056–2065) and are exacerbated in the long term (2091–2100).

The forcing scenario with the highest GHG emissions, SSP5-8.5, predicts the greatest changes in the mean value and the temporal variability of wind power density, regardless of the location. This scenario projects in the long-term future a general decrease of ~15% in the European wind power density, with an annual reduction of ~0.2%. As for the variability, a general increase of over 10% in the coefficient of variation of wind power density is predicted. On the other hand, the business-as-usual climate change scenario, SSP2-4.5, does not show a general trend in the European wind energy. Long-term changes in wind power density relative to historical data depend largely on the region, and can be either negative or positive.

Regardless of the climate change scenario, a remarkable increase in mean wind power density is located in West Finland, whereas considerable decreases are anticipated in the Central Mediterranean (centred in the Italian Peninsula and Tyrrhenian Sea), the northernmost regions of Continental Europe (centred in the Finnish Lapland) and the upper European Atlantic Ocean – in latitudes above 45°N, including Ireland, Britain and Iceland. Conversely, diametrically opposed predictions for different scenarios are located in much of Western and Central Europe (France, Belgium, the Netherlands, Germany, Czech Republic).

These results are of interest in assessing the potential of the wind energy sector in Europe, which is expected to develop further in the context of the European Union's Green Deal. It serves as a reference for future regional studies and downscaling initiatives of the CMIP6 focused on the effects of climate change on the available wind energy resource. Future works may assess whether locations with already well-developed wind power may see the resource decrease, whereas areas which have received less attention so far may become the object of future studies. These additional studies will become even more relevant with the rise of new technologies such as floating offshore wind, leading the sector to yet largely unexplored areas due to its rapid development.

This work consisted in a large-scale, high-level assessment, which may be seen as a first approximation to the study of the long-term trends of the European wind energy resource. Even though individual uncertainties are reduced by using a multi-model ensemble, the limitations of the GCMs involved in the CMIP6, including the coarse resolution, are inherited, which must be born in mind when considering localised areas in the vicinity of mountain ranges. In future, this study ought to be complemented with additional work on smaller scales.

CRediT authorship contribution statement

A. Martinez: Conceptualization, Methodology, Investigation, Data curation, Writing - original draft. **G. Iglesias:** Conceptualization, Methodology.

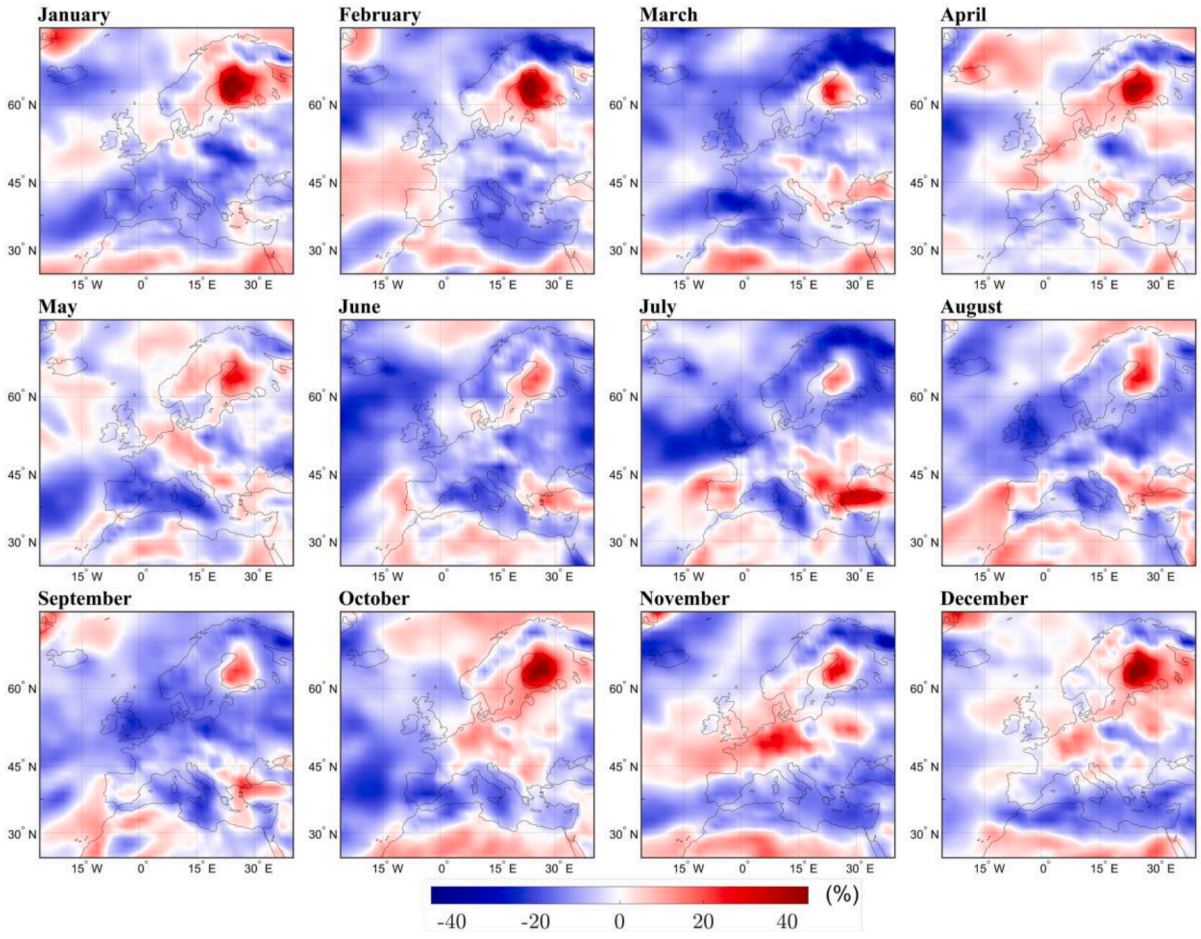

Fig. 11. Evolution (%) of the monthly mean wind power density in the mid-term future under SSP5-8.5 climate change scenario.

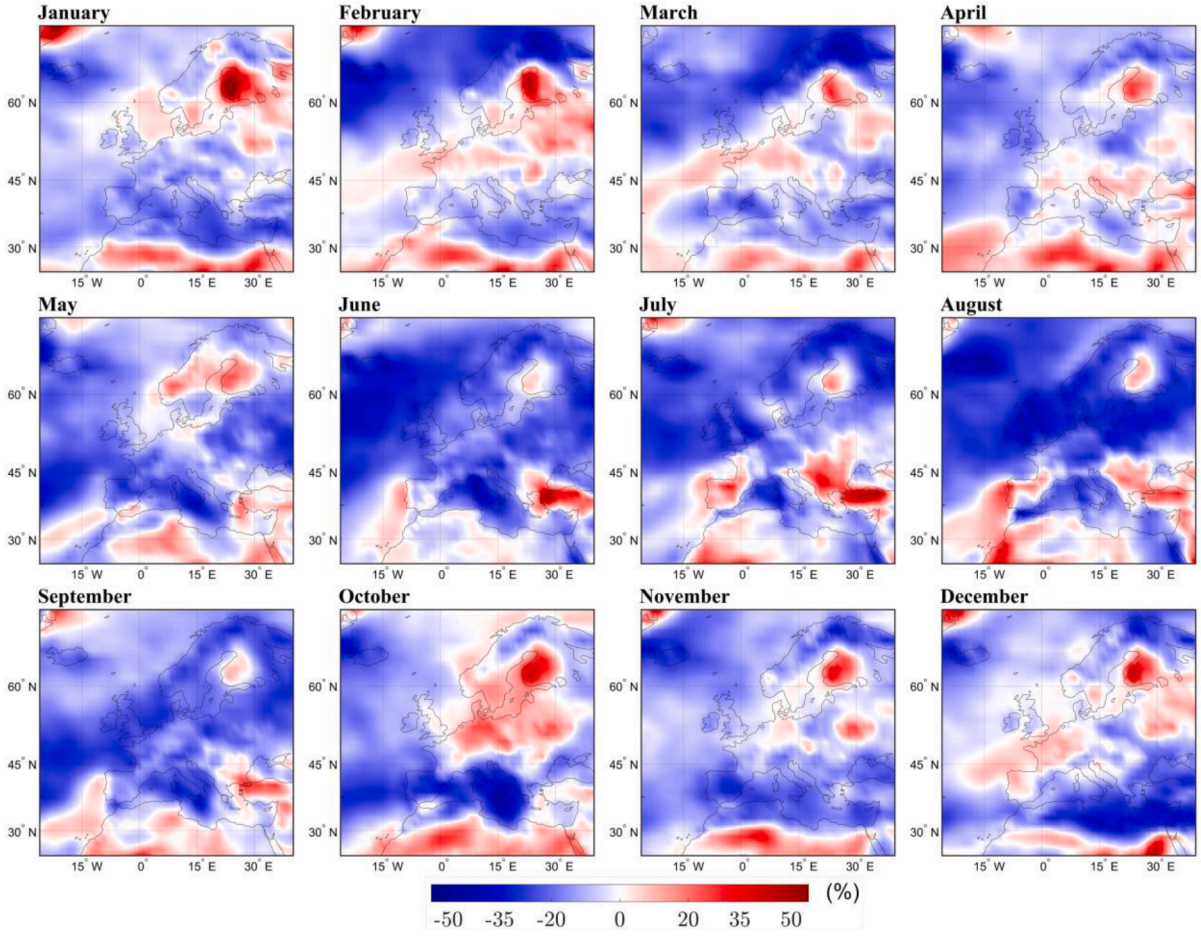

Fig. 12. Evolution (%) of the monthly mean wind power density in the long-term future under SSP5-8.5 climate change scenario.

Declaration of Competing Interest

The authors declare that they have no known competing financial interests or personal relationships that could have appeared to influence the work reported in this paper.

Acknowledgements

The first author is grateful for the support of Science Foundation Ireland (SFI) and MaREI, the Marine Renewable Energy Centre Ireland, grant SFI MAREI2_12/RC/2302/P2 Platform RA1b. The authors are also grateful to: the Working Group on Coupled Modelling of the World Climate Research Programme, which is responsible for the CMIP6, and the climate modelling groups involved in its activities, for producing and making available their model outputs; the Earth System Grid Federation (ESGF), for storing and providing access to the data; and the funding agencies supporting CMIP6 and ESGF.

References

[1] Stocker, T.F., D. Qin, G.-K. Plattner, M. Tignor, S.K. Allen, J. Boschung, A. Nauels, Y. Xia, V. Bex, and P.M. Midgley, Climate change 2013: The physical science basis. Contribution of working group I to the fifth assessment report of the intergovernmental panel on climate change, 2013. 1535.
[2] Komusanac, I., D. Fraile, and G. Brindley, Wind energy in Europe in 2019. Trends and statistics. WindEurope: Brussels, Belgium, 2020.
[3] Foundation, E.C., ROADMAP 2050; A Practical Guide to a Prosperous, Low-Carbon Europe. 2010.
[4] Enevoldsen, P., F.-H. Permien, I. Bakhtaoui, A.-K. von Krauland, M.Z. Jacobson, G. Xydis, B.K. Sovacool, S.V. Valentine, D. Luecht, and G. Oxley, How much wind power potential does europe have? Examining european wind power potential with an enhanced socio-technical atlas. Energy Policy, 2019. 132: p. 1092-1100.
[5] Ulazia A, Sáenz J, Ibarra-Berastegui G, González-Rojí SJ, Carreno-Madinabeitia S. Using 3DVAR data assimilation to measure offshore wind energy potential at different turbine heights in the West Mediterranean. Appl Energy 2017;208:1232–45.
[6] Perez-Collazo C, Greaves D, Iglesias G. Hydrodynamic response of the WEC sub-system of a novel hybrid wind-wave energy converter. Energy Convers Manage 2018;171:307–25.
[7] Perez-Collazo C, Pemberton R, Greaves D, Iglesias G. Monopile-mounted wave energy converter for a hybrid wind-wave system. Energy Convers Manage 2019;199.
[8] Perez-Collazo C, Greaves D, Iglesias G. A novel hybrid wind-wave energy converter for jacket-frame substructures. Energies 2018;11(3):637.
[9] Kabalci E. Design and analysis of a hybrid renewable energy plant with solar and wind power. Energy Convers Manage 2013;72:51–9.
[10] Baghdadi F, Mohammedi K, Diaf S, Behar O. Feasibility study and energy conversion analysis of stand-alone hybrid renewable energy system. Energy Convers Manage 2015;105:471–9.
[11] Astariz S, Perez-Collazo C, Abanades J, Iglesias G. Towards the optimal design of a co-located wind-wave farm. Energy 2015;84:15–24.
[12] Ramos V, Iglesias G. Wind power viability on a small island. Int J Green Energy 2014;11(7):741–60.
[13] Schallenberg-Rodríguez J, García Montesdeoca N. Spatial planning to estimate the offshore wind energy potential in coastal regions and islands. Practical case: The Canary Islands. Energy 2018;143:91–103.
[14] Fyrippis I, Axaopoulos PJ, Panayiotou G. Wind energy potential assessment in Naxos Island, Greece. Appl Energy 2010;87(2):577–86.
[15] Perez-Collazo C, Greaves D, Iglesias G. A review of combined wave and offshore wind energy. Renew Sustain Energy Rev 2015;42:141–53.
[16] Veigas M, Iglesias G. A hybrid wave-wind offshore farm for an island. Int J Green Energy 2015;12(6):570–6.
[17] Veigas M, Iglesias G. Wave and offshore wind potential for the island of Tenerife. Energy Convers Manage 2013;76:738–45.
[18] Veigas M, Iglesias G. Potentials of a hybrid offshore farm for the island of Fuerteventura. Energy Convers Manage 2014;86:300–8.
[19] Kaldellis JK, Kavadias K, Christinakis E. Evaluation of the wind–hydro energy solution for remote islands. Energy Convers Manage 2001;42(9):1105–20.

[20] Rockel B, Woth K. Extremes of near-surface wind speed over Europe and their future changes as estimated from an ensemble of RCM simulations. Clim Change 2007;81(1):267–80.
[21] Räisänen, J., U. Hansson, A. Ullerstig, R. Döscher, L. Graham, C. Jones, H. Meier, P. Samuelsson, and U. Willén, European climate in the late twenty-first century: regional simulations with two driving global models and two forcing scenarios. Climate dynamics, 2004. 22(1): p. 13-31.
[22] IPCC, Climate change 2001: the scientific basis. 2001, Cambridge University Press Cambridge, UK. p. 881.
[23] Pryor S, Barthelmie R, Kjellström E. Potential climate change impact on wind energy resources in northern Europe: analyses using a regional climate model. Clim Dyn 2005;25(7–8):815–35.
[24] Bloom A, Kotroni V, Lagouvardos K. Climate change impact of wind energy availability in the Eastern Mediterranean using the regional climate model PRECIS. Nat Hazards Earth Syst Sci 2008;8(6).
[25] Hueging H, Haas R, Born K, Jacob D, Pinto JG. Regional changes in wind energy potential over Europe using regional climate model ensemble projections. J Appl Meteorol Climatol 2013;52(4):903–17.
[26] Tobin I, Vautard R, Balog I, Bréon F-M, Jerez S, Ruti PM, Thais F, Vrac M, Yiou P. Assessing climate change impacts on European wind energy from ENSEMBLES high-resolution climate projections. Clim Change 2015;128(1–2):99–112.
[27] Cradden LC, Harrison GP, Chick JP. Will climate change impact on wind power development in the UK? Clim Change 2012;115(3–4):837–52.
[28] Nolan P, Lynch P, McGrath R, Semmler T, Wang S. Simulating climate change and its effects on the wind energy resource of Ireland. Wind Energy 2012;15(4): 593–608.
[29] Nolan P, Lynch P, Sweeney C. Simulating the future wind energy resource of Ireland using the COSMO-CLM model. Wind Energy 2014;17(1):19–37.
[30] Carvalho D, Rocha A, Gómez-Gesteira M, Silva Santos C. Potential impacts of climate change on European wind energy resource under the CMIP5 future climate projections. Renewable Energy 2017;101:29–40.
[31] Reyers M, Moemken J, Pinto JG. Future changes of wind energy potentials over Europe in a large CMIP5 multi-model ensemble. Int J Climatol 2016;36(2):783–96.
[32] Moss RH, Edmonds JA, Hibbard KA, Manning MR, Rose SK, Van Vuuren DP, Carter TR, Emori S, Kainuma M, Kram T. The next generation of scenarios for climate change research and assessment. Nature 2010;463(7282):747–56.
[33] Eyring V, Bony S, Meehl GA, Senior CA, Stevens B, Stouffer RJ, Taylor KE. Overview of the Coupled Model Intercomparison Project Phase 6 (CMIP6) experimental design and organization. Geosci Model Dev 2016;9(5):1937–58.
[34] O'Neill, B.C., C. Tebaldi, D.P. Van Vuuren, V. Eyring, P. Friedlingstein, G. Hurtt, R. Knutti, E. Kriegler, J.-F. Lamarque, and J. Lowe, The scenario model intercomparison project (ScenarioMIP) for CMIP6. 2016.
[35] O'Neill BC, Kriegler E, Ebi KL, Kemp-Benedict E, Riahi K, Rothman DS, van Ruijven BJ, van Vuuren DP, Birkmann J, Kok K. The roads ahead: narratives for shared socioeconomic pathways describing world futures in the 21st century. Global Environ Change 2017;42:169–80.
[36] Riahi, K., D.P. Van Vuuren, E. Kriegler, J. Edmonds, B.C. O'neill, S. Fujimori, N. Bauer, K. Calvin, R. Dellink, and O. Fricko, The shared socioeconomic pathways and their energy, land use, and greenhouse gas emissions implications: an overview. Global Environmental Change, 2017. 42: p. 153-168.
[37] Zappa G, Shaffrey L, Hodges K, Sansom PG, Stephenson DB. A multimodel assessment of future projections of North Atlantic and European extratropical cyclones in the CMIP5 climate models. J. Climate. 2013;26:5846–62.
[38] Bansal RC, Bhatti TS, Kothari DP. On some of the design aspects of wind energy conversion systems. Energy Convers Manage 2002;43(16):2175–87.
[39] Kulkarni S, Huang H-P. Changes in surface wind speed over North America from CMIP5 model projections and implications for wind energy. Adv Meteorol 2014; 2014.
[40] Semmler, T., S. Danilov, T. Rackow, D. Sidorenko, D. Barbi, J. Hegewald, H.K. Pradhan, D. Sein, Q. Wang, and T. Jung, AWI AWI-CM1.1MR model output prepared for CMIP6 ScenarioMIP. 2019, Earth System Grid Federation.
[41] Xin, X., T. Wu, X. Shi, F. Zhang, J. Li, M. Chu, Q. Liu, J. Yan, Q. Ma, and M. Wei, BCC BCC-CSM2MR model output prepared for CMIP6 ScenarioMIP. 2019, Earth System Grid Federation.
[42] Yu, Y., CAS FGOALS-f3-L model output prepared for CMIP6 ScenarioMIP. 2019, Earth System Grid Federation.
[43] Swart, N.C., J.N.S. Cole, V.V. Kharin, M. Lazare, J.F. Scinocca, N.P. Gillett, J. Anstey, V. Arora, J.R. Christian, Y. Jiao, W.G. Lee, F. Majaess, O.A. Saenko, C. Seiler, C. Seinen, A. Shao, L. Solheim, K. von Salzen, D. Yang, B. Winter, and M. Sigmond, CCCma CanESM5 model output prepared for CMIP6 ScenarioMIP. 2019, Earth System Grid Federation.
[44] Dix, M., D. Bi, P. Dobrohotoff, R. Fiedler, I. Harman, R. Law, C. Mackallah, S. Marsland, S. O'Farrell, H. Rashid, J. Srbinovsky, A. Sullivan, C. Trenham, P. Vohralik, I. Watterson, G. Williams, M. Woodhouse, R. Bodman, F.B. Dias, C. Domingues, N. Hannah, A. Heerdegen, A. Savita, S. Wales, C. Allen, K. Druken, B. Evans, C. Richards, S.M. Ridzwan, D. Roberts, J. Smillie, K. Snow, M. Ward, and R. Yang, CSIRO-ARCCSS ACCESS-CM2 model output prepared for CMIP6 ScenarioMIP. 2019, Earth System Grid Federation.
[45] Schupfner, M., K.-H. Wieners, F. Wachsmann, C. Steger, M. Bittner, J. Jungclaus, B. Früh, K. Pankatz, M. Giorgetta, C. Reick, S. Legutke, M. Esch, V. Gayler, H. Haak, P. de Vrese, T. Raddatz, T. Mauritsen, J.-S. von Storch, J. Behrens, V. Brovkin, M. Claussen, T. Crueger, I. Fast, S. Fiedler, S. Hagemann, C. Hohenegger, T. Jahns, S. Kloster, S. Kinne, G. Lasslop, L. Kornblueh, J. Marotzke, D. Matei, K. Meraner, U. Mikolajewicz, K. Modali, W. Müller, J. Nabel, D. Notz, K. Peters, R. Pincus, H. Pohlmann, J. Pongratz, S. Rast, H. Schmidt, R. Schnur, U. Schulzweida, K. Six, B. Stevens, A. Voigt, and E. Roeckner, DKRZ MPI-ESM1.2-HR model output prepared for CMIP6 ScenarioMIP. 2019, Earth System Grid Federation.
[46] Wieners, K.-H., M. Giorgetta, J. Jungclaus, C. Reick, M. Esch, M. Bittner, V. Gayler, H. Haak, P. de Vrese, T. Raddatz, T. Mauritsen, J.-S. von Storch, J. Behrens, V. Brovkin, M. Claussen, T. Crueger, I. Fast, S. Fiedler, S. Hagemann, C. Hohenegger, T. Jahns, S. Kloster, S. Kinne, G. Lasslop, L. Kornblueh, J. Marotzke, D. Matei, K. Meraner, U. Mikolajewicz, K. Modali, W. Müller, J. Nabel, D. Notz, K. Peters, R. Pincus, H. Pohlmann, J. Pongratz, S. Rast, H. Schmidt, R. Schnur, U. Schulzweida, K. Six, B. Stevens, A. Voigt, and E. Roeckner, MPI-M MPI-ESM1.2-LR model output prepared for CMIP6 ScenarioMIP ssp245. 2019, Earth System Grid Federation.
[47] Wieners, K.-H., M. Giorgetta, J. Jungclaus, C. Reick, M. Esch, M. Bittner, V. Gayler, H. Haak, P. de Vrese, T. Raddatz, T. Mauritsen, J.-S. von Storch, J. Behrens, V. Brovkin, M. Claussen, T. Crueger, I. Fast, S. Fiedler, S. Hagemann, C. Hohenegger, T. Jahns, S. Kloster, S. Kinne, G. Lasslop, L. Kornblueh, J. Marotzke, D. Matei, K. Meraner, U. Mikolajewicz, K. Modali, W. Müller, J. Nabel, D. Notz, K. Peters, R. Pincus, H. Pohlmann, J. Pongratz, S. Rast, H. Schmidt, R. Schnur, U. Schulzweida, K. Six, B. Stevens, A. Voigt, and E. Roeckner, MPI-M MPI-ESM1.2-LR model output prepared for CMIP6 ScenarioMIP ssp585. 2019, Earth System Grid Federation.
[48] Consortium, E.C.-E., EC-Earth-Consortium EC-Earth3 model output prepared for CMIP6 ScenarioMIP. 2019, Earth System Grid Federation.
[49] Volodin, E., E. Mortikov, A. Gritsun, V. Lykossov, V. Galin, N. Diansky, A. Gusev, S. Kostrykin, N. Iakovlev, A. Shestakova, and S. Emelina, INM INM-CM4-8 model output prepared for CMIP6 ScenarioMIP ssp245. 2019, Earth System Grid Federation.
[50] Volodin, E., E. Mortikov, A. Gritsun, V. Lykossov, V. Galin, N. Diansky, A. Gusev, S. Kostrykin, N. Iakovlev, A. Shestakova, and S. Emelina, INM INM-CM4-8 model output prepared for CMIP6 ScenarioMIP ssp585. 2019, Earth System Grid Federation.
[51] Volodin, E., E. Mortikov, A. Gritsun, V. Lykossov, V. Galin, N. Diansky, A. Gusev, S. Kostrykin, N. Iakovlev, A. Shestakova, and S. Emelina, INM INM-CM5-0 model output prepared for CMIP6 ScenarioMIP ssp245. 2019, Earth System Grid Federation.
[52] Volodin, E., E. Mortikov, A. Gritsun, V. Lykossov, V. Galin, N. Diansky, A. Gusev, S. Kostrykin, N. Iakovlev, A. Shestakova, and S. Emelina, INM INM-CM5-0 model output prepared for CMIP6 ScenarioMIP ssp585. 2019, Earth System Grid Federation.
[53] Boucher, O., S. Denvil, A. Caubel, and M.A. Foujols, IPSL IPSL-CM6A-LR model output prepared for CMIP6 ScenarioMIP. 2019, Earth System Grid Federation.
[54] Shiogama, H., M. Abe, and H. Tatebe, MIROC MIROC6 model output prepared for CMIP6 ScenarioMIP. 2019, Earth System Grid Federation.
[55] Yukimoto, S., T. Koshiro, H. Kawai, N. Oshima, K. Yoshida, S. Urakawa, H. Tsujino, M. Deushi, T. Tanaka, M. Hosaka, H. Yoshimura, E. Shindo, R. Mizuta, M. Ishii, A. Obata, and Y. Adachi, MRI MRI-ESM2.0 model output prepared for CMIP6 ScenarioMIP. 2019, Earth System Grid Federation.
[56] Danabasoglu, G., NCAR CESM2-WACCM model output prepared for CMIP6 ScenarioMIP. 2019, Earth System Grid Federation.
[57] Bentsen, M., D.J.L. Oliviè, Ø. Seland, T. Toniazzo, A. Gjermundsen, L.S. Graff, J.B. Debernard, A.K. Gupta, Y. He, A. Kirkevåg, J. Schwinger, J. Tjiputra, K.S. Aas, I. Bethke, Y. Fan, J. Griesfeller, A. Grini, C. Guo, M. Ilicak, I.H.H. Karset, O.A. Landgren, J. Liakka, K.O. Moseid, A. Nummelin, C. Spensberger, H. Tang, Z. Zhang, C. Heinze, T. Iversen, and M. Schulz, NCC NorESM2-MM model output prepared for CMIP6 CMIP. 2019, Earth System Grid Federation.
[58] Byun, Y.-H., Y.-J. Lim, S. Shim, H.M. Sung, M. Sun, J. Kim, B.-H. Kim, J.-H. Lee, and H. Moon, NIMS-KMA KACE1.0-G model output prepared for CMIP6 ScenarioMIP. 2019, Earth System Grid Federation.
[59] Guo, H., J.G. John, C. Blanton, C. McHugh, S. Nikonov, A. Radhakrishnan, N.T. Zadeh, V. Balaji, J. Durachta, C. Dupuis, R. Menzel, T. Robinson, S. Underwood, H. Vahlenkamp, K.A. Dunne, P.P.G. Gauthier, P. Ginoux, S.M. Griffies, R. Hallberg, M. Harrison, W. Hurlin, P. Lin, S. Malyshev, V. Naik, F. Paulot, D.J. Paynter, J. Ploshay, D.M. Schwarzkopf, C.J. Seman, A. Shao, L. Silvers, B. Wyman, X. Yan, Y. Zeng, A. Adcroft, J.P. Dunne, I.M. Held, J.P. Krasting, L.W. Horowitz, C. Milly, E. Shevliakova, M. Winton, M. Zhao, and R. Zhang, NOAA-GFDL GFDL-CM4 model output prepared for CMIP6 ScenarioMIP. 2018, Earth System Grid Federation.
[60] John, J.G., C. Blanton, C. McHugh, A. Radhakrishnan, K. Rand, H. Vahlenkamp, C. Wilson, N.T. Zadeh, P.P.G. Gauthier, J.P. Dunne, R. Dussin, L.W. Horowitz, P. Lin, S. Malyshev, V. Naik, J. Ploshay, L. Silvers, C. Stock, M. Winton, and Y. Zeng, NOAA-GFDL GFDL-ESM4 model output prepared for CMIP6 ScenarioMIP. 2018, Earth System Grid Federation.
[61] Hersbach H, Dee D. ERA5 reanalysis is in production. ECMWF newsletter 2016;147 (7):5–6.
[62] Ulazia A, Sáenz J, Ibarra-Berastegi G, González-Rojí SJ, Carreno-Madinabeitia S. Global estimations of wind energy potential considering seasonal air density changes. Energy 2019;187.
[63] Gutowski, W.J., F. Giorgi, B. Timbal, A. Frigon, D. Jacob, H.-S. Kang, K. Raghavan, B. Lee, C. Lennard, and G. Nikulin, WCRP coordinated regional downscaling experiment (CORDEX): a diagnostic MIP for CMIP6. 2016.
[64] Dosio A, Panitz H-J, Schubert-Frisius M, Lüthi D. Dynamical downscaling of CMIP5 global circulation models over CORDEX-Africa with COSMO-CLM: evaluation over the present climate and analysis of the added value. Clim Dyn 2015;44(9–10): 2637–61.
[65] Wilks, D.S., Statistical methods in the atmospheric sciences. Vol. 100. 2011: Academic press.
[66] Jones PW. First-and second-order conservative remapping schemes for grids in spherical coordinates. Mon Weather Rev 1999;127(9):2204–10.

[67] Brands S, Herrera S, Fernández J, Gutiérrez JM. How well do CMIP5 Earth System Models simulate present climate conditions in Europe and Africa? Clim Dyn 2013; 41(3–4):803–17.
[68] Pierce DW, Barnett TP, Santer BD, Gleckler PJ. Selecting global climate models for regional climate change studies. Proc Natl Acad Sci 2009;106(21):8441–6.
[69] Räisänen J, Palmer T. A probability and decision-model analysis of a multimodel ensemble of climate change simulations. J Clim 2001;14(15):3212–26.
[70] Tebaldi C, Knutti R. The use of the multi-model ensemble in probabilistic climate projections. Philos Trans Royal Society A: Math Phys Eng Sci 1857;2007(365): 2053–75.
[71] Rusu E. An evaluation of the wind energy dynamics in the Baltic Sea, past and future projections. Renewable Energy 2020;160:350–62.
[72] Walpole, R.E., R.H. Myers, S.L. Myers, and K. Ye, Probability and statistics for engineers and scientists. Vol. 5. 1993: Macmillan New York.